Open access • Journal Article • DOI:10.1039/C4EE01914H

Stabilization of n-cadmium telluride photoanodes for water oxidation to O2(g) in aqueous alkaline electrolytes using amorphous TiO2 films formed by atomic-layer deposition — Source link

Michael F. Lichterman, Azhar I. Carim, Matthew T. McDowell, Shu Hu ...+3 more authors

Institutions: California Institute of Technology

Published on: 17 Sep 2014 - Energy and Environmental Science (Royal Society of Chemistry)

Topics: Amorphous solid, Photoelectrochemical oxidation, Cadmium telluride photovoltaics, Passivation and Atomic layer deposition

Energy & Environmental Science

COMMUNICATION

View Article Online
View Journal | View Issue

Cite this: *Energy Environ. Sci.*, 2014, 7, 3334

Received 20th June 2014
Accepted 21st August 2014

DOI: 10.1039/c4ee01914h

www.rsc.org/ees

Stabilization of n-cadmium telluride photoanodes for water oxidation to O_2(g) in aqueous alkaline electrolytes using amorphous TiO_2 films formed by atomic-layer deposition†

Michael F. Lichterman,[ab] Azhar I. Carim,[a] Matthew T. McDowell,[ab] Shu Hu,[ab] Harry B. Gray,*[ac] Bruce S. Brunschwig*[c] and Nathan S. Lewis*[abcd]

Although II–VI semiconductors such as CdS, CdTe, CdSe, ZnTe, and alloys thereof can have nearly ideal band gaps and band-edge positions for the production of solar fuels, II–VI photoanodes are well-known to be unstable towards photocorrosion or photopassivation when in contact with aqueous electrolytes. Atomic-layer deposition (ALD) of amorphous, "leaky" TiO_2 films coated with thin films or islands of Ni oxide has been shown to robustly protect Si, GaAs, and other III–V materials from photocorrosion and therefore to facilitate the robust, solar-driven photoelectrochemical oxidation of H_2O to O_2(g). We demonstrate herein that ALD-deposited 140 nm thick amorphous TiO_2 films also effectively protect single crystalline n-CdTe photoanodes from corrosion or passivation. An n-CdTe/TiO_2 electrode with a thin overlayer of a Ni-oxide based oxygen-evolution electrocatalyst produced 435 ± 15 mV of photovoltage with a light-limited current density of 21 ± 1 mA cm^{-2} under 100 mW cm^{-2} of simulated Air Mass 1.5 illumination. The ALD-deposited TiO_2 films are highly optically transparent and electrically conductive. We show that an n-CdTe/TiO_2/Ni oxide electrode enables the stable solar-driven oxidation of H_2O to O_2(g) in strongly alkaline aqueous solutions, where passive, intrinsically safe, efficient systems for solar-driven water splitting can be operated.

Broader context

High-efficiency photoelectrochemical (PEC) solar-driven water splitting and/or carbon dioxide reduction will require the use of semiconductors capable of delivering a substantial amount of current as well as the photovoltage required to drive the fuel-forming anodic and cathodic half-reactions, respectively. Although metal oxides have received much attention as photoanodes due to their stability against oxidation, such systems generally suffer from low maximum photocurrent densities in sunlight due to the large band gaps of the materials explored to date. Semiconductors with smaller band gaps, such as CdTe, are better matched to the solar spectrum and have more suitable valence-band positions; however, such materials are generally unstable in aqueous electrolytes under photoanodic conditions. We demonstrate herein that atomic-layer deposition of amorphous TiO_2 films forms a protection layer on n-CdTe photoanodes that, with a Ni-oxide based electrocatalyst layer, allows for photocatalytic water oxidation at the electrolyte interface. Such n-CdTe/TiO_2/Ni oxide photoanodes yielded quantitative oxidation of water to O_2(g) with internal quantum yields approaching unity for extended periods of operation under 100 mW cm^{-2} of simulated solar illumination.

CdTe, with a 1.44 eV band gap, has been widely studied since the 1980s,[1–6] and is currently used primarily in thin-film solar cells in which p-CdTe is deposited upon n-CdS to form a buried heterojunction device.[7,8] CdTe has furthermore been investigated for use in photoelectrochemical (PEC) applications but is known to undergo a number of facile photooxidation or photocorrosion processes in various aqueous, as well as organic, media.[1,2] Strongly alkaline or strongly acidic media have numerous benefits for the electrolysis of water due to their high conductivity without the need for added electrolyte or buffering species and minimal pH gradients under operating conditions. Further, at high and low pH, viable permselective ionophoric membranes are available to separate the products of electrolysis, and the kinetics of water oxidation with suitable electrocatalysts is rapid, thus making possible the construction of a passive, intrinsically safe and efficient solar-driven water-splitting device.[9–11] However, efficient photoanodes typically are unstable and rapidly corrode or passivate when operated in contact with electrolytes in these pH ranges.[12,13] Recently, several reports have been published in which the protection of otherwise unstable materials is carried out using a protecting layer such as TiO_2, MnO or metal-modified In-doped SnO_2.[14–16] Facile electron conduction is expected through the conduction band of TiO_2, and hence TiO_2 has been developed as a

[a]*Division of Chemistry and Chemical Engineering, California Institute of Technology, Pasadena, CA 91125, USA*

[b]*The Joint Center for Artificial Photosynthesis, California Institute of Technology, Pasadena, CA 91125, USA. E-mail: nslewis@caltech.edu; Fax: 626-395-8867; Tel: 626-395-6335*

[c]*Beckman Institute, California Institute of Technology, Pasadena, CA 91125, USA*

[d]*Kavli Nanoscience Institute, California Institute of Technology, Pasadena, CA 91125, USA*

† Electronic supplementary information (ESI) available: Detailed experimental methods, SEM/EDS data, XPS data, and other photoelectrochemical information are available. See DOI: 10.1039/c4ee01914h

protection layer for photocathodes. In contrast, stoichiometric TiO_2 should present a tunnel barrier to photogenerated holes at energies near that required for water oxidation. We report herein that 140 nm thick amorphous TiO_2 films deposited by atomic-layer deposition (ALD) and modified by the addition of a Ni oxide catalytic layer effectively protect n-CdTe photoanodes from corrosion or passivation and effect the quantitative oxidation of H_2O to O_2(g). Protected n-CdTe photoanodes produced 435 ± 15 mV of photovoltage and light-limited current densities of 21 ± 1 mA cm^{-2} under 100 mW cm^{-2} of simulated Air Mass (AM)1.5 illumination.

Atomic-layer deposition (ALD) was utilized to deposit films of TiO_2 up to 150 nm in thickness on (111)-oriented n-CdTe samples with a carrier concentration of 1×10^{17} cm^{-3}. The electrical characteristics of such films have been described previously.[12] A thin film of Ni was then deposited by sputtering. Upon oxidation, the Ni layer produces an earth-abundant, highly active, low overpotential Ni oxide electrocatalyst for the oxygen-evolution reaction (OER).[12] Fig. 1 shows a representative cross-sectional scanning-electron micrograph of a resulting photoelectrode.

Fig. 2 shows typical current density *vs.* potential (*J–E*) data for (a) an n-CdTe/TiO_2/Ni photoanode in pH = 14 KOH(aq) plotted against the reversible hydrogen electrode potential, RHE,‡ and (b) an n-CdTe/TiO_2/Ni photoanode in contact with an aqueous ferro/ferricyanide solution (KCl, $Fe(CN)_6^{3-}$, and $Fe(CN)_6^{4-}$, of 1.00, 0.05, and 0.35 M concentrations, respectively), both under 100 mW cm^{-2} of simulated AM1.5 illumination (Xenon lamp with an AM1.5 filter set). Unetched samples exhibited lower photovoltages and low fill factors (Fig. S1†), whereas samples etched for 30 s in Br_2/CH_3OH produced superior fill factors, high photocurrents and improved photovoltages. Etching concentrations in the range of 0.1% to 1% Br_2/CH_3OH produced the most optimized photoelectrodes from the n-CdTe wafer used in this study. Open-circuit photovoltages of approximately 435 mV and light-limited photocurrent densities of 21 mA cm^{-2} were observed for n-CdTe/TiO_2/Ni photoanodes in pH = 14 KOH (aq) as well as in contact with the aqueous ferri/ferrocyanide solutions (Fig. 2). For comparison, a similarly protected n-Si photoanode has been shown to provide 28 mA cm^{-2} of light-limited photocurrent density and 410 mV of photovoltage, a similarly protected n-GaP photoanode has been shown to provide a light-limited photocurrent of 3.4 mA cm^{-2} and 590 mV of photovoltage, and a similarly protected gallium arsenide photoanode containing a buried junction, np^+–GaAs, has been shown to provide photocurrent densities of 14.3 mA cm^{-2} and photovoltages of 810 mV.[12] To provide perspective on the performance produced provided by the protection scheme, load-line analysis indicated that obtaining the observed *J–E* performance of the n-CdTe/TiO_2/Ni photoanode using a Si photovoltaic (PV) cell electrically in series with an electrocatalytic anode that exhibited virtually identical *J–E* behavior to that of a 2 nm Ni film on a Ti electrode[17] would require the use of a 7.5% efficient Si PV cell with an open-circuit voltage of 0.48 V, a short-circuit photocurrent density of 22 mA cm^{-2}, and a fill factor of 0.71.

Scanning-electron microscopy (SEM) and energy-dispersive X-ray spectroscopy (EDS) were used to further analyze the n-CdTe/TiO_2/Ni interface. As shown in the cross-sectional micrograph (Fig. 1), the thickness of the TiO_2 layer was 140 nm, which implies a growth rate of 0.056 nm per cycle for the 2500 cycle

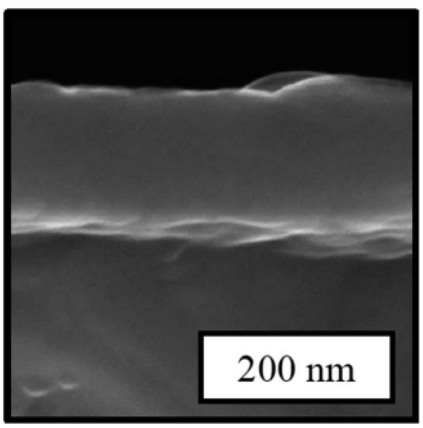

Fig. 1 Representative cross-sectional scanning electron micrograph of an n-CdTe/TiO_2/Ni electrode depicting the ALD-grown TiO_2 film above the n-CdTe wafer section. The Ni deposited onto the TiO_2 is not visible in this micrograph but was detected by EDS (see ESI Fig. S3†).

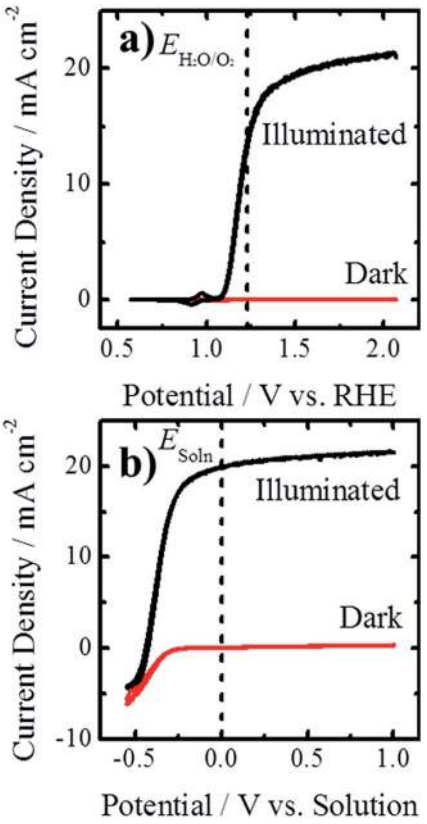

Fig. 2 *J–E* data obtained with a n-CdTe/TiO_2/Ni electrode in the dark and under illumination in (a) pH = 14 KOH(aq) and (b) a $Fe(CN)_6^{3-/4-}$ solution. Illumination was provided by a Xenon arc lamp with an AM1.5 filter set and the light intensity was calibrated to 100 mW cm^{-2} of AM1.5G illumination using a secondary standard calibrated Si solar cell.

TiO_2 sample. Fig. S2 and Table S1† show the EDS data obtained at various locations in the n-CdTe/TiO_2/Ni structure. Notably, the EDS data indicated that a slightly Cd-poor region was present at the interface, as would be expected for an oxidizing etch that produced an acceptor-rich interface. This behavior suggests that the interfacial layer is key to producing the photovoltage exhibited by these samples, and agrees well with prior suggestions that such etches form an acceptor-rich, Cd-poor surface at the CdTe interface[18] which pins the photovoltage to ~0.5 V under similar illumination conditions.[19]

XPS experiments were performed to characterize the surface properties of the etched n-CdTe wafers prior to the ALD of the TiO_2 overlayer. An unetched wafer showed nearly equal amounts of Te and Cd at the surface, in addition to a substantial amount of tellurium oxide (Fig. S3 and Table S2†), whereas the Br_2/CH_3OH-etched samples had a 0.75 : 1 ratio of cadmium to tellurium at the surface and exhibited a much smaller tellurium oxide peak. This ratio suggests the formation of a p-type layer at the surface of the n-CdTe wafer, which influences the magnitude of the observed photovoltages. Brief (15 s) Ar^+ sputter-etching between XPS acquisitions quickly returned the Te : Cd ratio to unity before leading to a Cd-rich surface, due to the different sputter-etching rates of tellurium and cadmium. While the different sputter-etching rates made rigorous depth profiling difficult using this experimental technique, these results show that the Br_2/CH_3OH etch only created this p-type layer within a very narrow layer at the surface, with a depth on the order of nanometers.

The spectral response data for n-CdTe/TiO_2/Ni electrodes indicated a high quantum yield for water oxidation (Fig. 3), with minimal absorption of light by the TiO_2/Ni overlayers. Spectral response measurements were undertaken at 2.07 V *vs.* RHE; this potential was chosen as it allowed for a large photocurrent to be effected (*i.e.* light-limited current density). Based on integration of the spectral response data with the wavelength-dependent irradiance of the AM1.5G solar spectrum, the sample etched with 1% Br_2 in CH_3OH resulted in photoelectrodes that exhibited excellent quantum yields in lower-wavelength regions, as well as high quantum yields at long wavelengths. Integration of the wavelength-dependent quantum yield of such electrodes with respect to the spectral irradiance distribution of the AM1.5G solar spectrum produced a light-limited photocurrent density of 20.5 mA cm^{-2}, which compared well with the observed value of 21.5 mA cm^{-2} (Fig. 2) at 2.07 V *vs.* RHE.

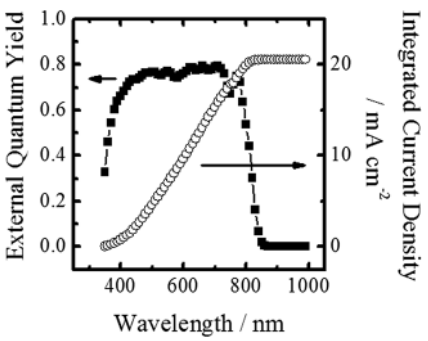

Fig. 3 External quantum yield for an n-CdTe/TiO_2/Ni electrode biased at 2.07 V *vs.* RHE in pH = 14 KOH(aq) solution and derived current density from integration against the AM1.5G spectrum.

Similar to the behavior of n-Si/TiO_2/Ni photoelectrodes,[8] n-CdTe/TiO_2/Ni photoelectrodes were stable for >100 hours of continuous operation during photoanodic current flow (Fig. 4a). An n-CdTe sample etched in the same manner but with only Ni deposited by sputtering, in the absence of ALD TiO_2, exhibited a decay in performance of ~40% over this same period of operation (Fig. S4†). Fig. S5† shows a comparison of the *J–E* behavior before and after 4 h of potentiostatic electrolysis at 2.07 V *vs.* RHE. The n-CdTe/TiO_2/Ni electrode remained effectively unchanged whereas both the photocurrent density and fill factor of an n-CdTe/Ni electrode decayed substantially over the same time period. Approximately 20 times more holes were passed through the circuit over 100 h than atoms present in the entire CdTe electrode, which strongly suggests that the photocurrent shown in Fig. 4a was predominantly associated with the faradaic oxidation of H_2O to O_2. Direct verification of this hypothesis was obtained using an oxygen detector,[20] which revealed that n-CdTe/TiO_2/Ni samples

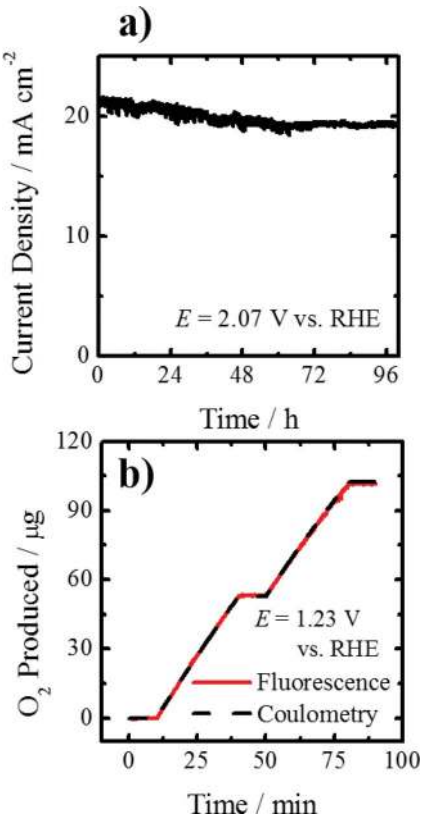

Fig. 4 (a) Current density as a function of time during potentiostatic electrolysis at 2.07 V *vs.* RHE in pH = 14 KOH(aq). (b) Oxygen production detected by a fluorescent probe and derived from coulometry during constant potential electrolysis at 1.23 V *vs.* RHE in pH = 14 KOH(aq). In (a), the n-CdTe/TiO_2/Ni electrode was illuminated by a Xenon arc lamp that had been calibrated to provide 100 mW cm^{-2} of simulated AM1.5G illumination; in (b), 20 mW cm^{-2} was used to prevent bubble formation.

operated in pH = 14 KOH(aq) (see ESI† for details) produced an amount of O_2 detected by the probe that was within experimental error of the amount of O_2 calculated based on the coulometry assuming 100% faradaic efficiency for O_2 production (Fig. 4b). The flat regions in the data before, in between, and after the measurement of photocurrent, and the time evolution of the detected O_2, correlated completely with the photoanodic current flow for two 30 min periods, strongly indicating that the detected O_2 was the result of water oxidation by the photoanode.

The amorphous TiO_2 coatings prepared by ALD yield buried junctions in which the semiconductor surface is protected from corrosion or passivation by the contacting electrolyte. The photovoltage of systems that do not contain a n–p^+ type base-emitter buried junction, such as n-CdTe/TiO_2/Ni electrodes, could be improved further through chemical control over the energetics at the semiconductor/oxide interface, including the introduction of surface dipoles, band-edge engineering, and other approaches to reduce the majority-carrier currents in the device. Nevertheless, this work shows that CdTe, generally believed to be unstable and not suited for investigation as a photoanode for the oxidation of water to O_2(g), can be beneficially used at least on the laboratory time scale for such purposes. Experiments are currently underway to quantify the methods by which the photovoltage and electrode stability can be further optimized in such systems.

Acknowledgements

This material is based upon work performed by the Joint Center for Artificial Photosynthesis, a DOE Energy Innovation Hub, supported through the Office of Science of the U. S. Department of Energy under Award Number DE-SC0004993. The authors gratefully acknowledge Dr Ke Sun for insightful discussions and Dr Slobodan Mitrovic for assistance collecting XPS data. AIC is grateful to the National Science Foundation for support from an NSF Graduate Research Fellowship. BSB and HBG acknowledge the Beckman Institute Materials and Laser Resource Centers and NSF CHE-1305124 for support.

Notes and references

‡ $E_{RHE} = E_{NHE} + 0.059 \times pH = E_{Ag/AgCl} + 0.197 + 0.059 \times pH$. At any pH, water oxidation at STP occurs at 1.23 V *vs.* RHE.

1 D. Lincot and J. Vedel, *J. Cryst. Growth*, 1985, **72**, 426–431.
2 J. S. Curran, *J. Electrochem. Soc.*, 1980, **127**, 2063–2067.
3 X. Mathew, J. P. Enriquez, A. Romeo and A. N. Tiwari, *Sol. Energy*, 2004, **77**, 831–838.
4 K. C. Mandal, S. Basu and D. N. Bose, *Bull. Mater. Sci.*, 1988, **10**, 349–351.
5 D. Liu, Z. Zheng, C. Wang, Y. Yin, S. Liu, B. Yang and Z. Jiang, *J. Phys. Chem. C*, 2013, **117**, 26529–26537.
6 Q. Li, Y. Yang, M. Sun, Y. Mu, W. Fu, H. Yang and L. Tian, *CrystEngComm*, 2013, **15**, 6911–6917.
7 S. G. Kumar and K. S. R. K. Rao, *Energy Environ. Sci.*, 2014, **7**, 45–102.
8 A. Romeo, M. Terheggen, D. Abou-Ras, D. L. Bätzner, F. J. Haug, M. Kälin, D. Rudmann and A. N. Tiwari, *Prog. Photovolt: Res. App.*, 2004, **12**, 93–111.
9 S. Haussener, C. Xiang, J. M. Spurgeon, S. Ardo, N. S. Lewis and A. Z. Weber, *Energy Environ. Sci.*, 2012, **5**, 9922–9935.
10 G. Merle, M. Wessling and K. Nijmeijer, *J. Membr. Sci.*, 2011, **377**, 1–35.
11 E. A. Hernandez-Pagan, N. M. Vargas-Barbosa, T. Wang, Y. Zhao, E. S. Smotkin and T. E. Mallouk, *Energy Environ. Sci.*, 2012, **5**, 7582–7589.
12 S. Hu, M. R. Shaner, J. A. Beardslee, M. Lichterman, B. S. Brunschwig and N. S. Lewis, *Science*, 2014, **344**, 1005–1009.
13 M. G. Walter, E. L. Warren, J. R. McKone, S. W. Boettcher, Q. Mi, E. A. Santori and N. S. Lewis, *Chem. Rev.*, 2010, **110**, 6446–6473.
14 B. Seger, D. S. Tilley, T. Pedersen, P. C. K. Vesborg, O. Hansen, M. Gratzel and I. Chorkendorff, *RSC Adv.*, 2013, **3**, 25902–25907.
15 N. C. Strandwitz, D. J. Comstock, R. L. Grimm, A. C. Nichols-Nielander, J. Elam and N. S. Lewis, *J. Phys. Chem. C*, 2013, **117**, 4931–4936.
16 K. Sun, S. Shen, J. S. Cheung, X. Pang, N. Park, J. Zhou, Y. Hu, Z. Sun, S. Y. Noh, C. T. Riley, P. K. L. Yu, S. Jin and D. Wang, *Phys. Chem. Chem. Phys.*, 2014, **16**, 4612–4625.
17 M. R. Shaner, K. T. Fountaine and H.-J. Lewerenz, *Appl. Phys. Lett.*, 2013, **103**, 143905.
18 H. S. White, A. J. Ricco and M. S. Wrighton, *J. Phys. Chem.*, 1983, **87**, 5140–5150.
19 S. Tanaka, J. A. Bruce and M. S. Wrighton, *J. Phys. Chem.*, 1981, **85**, 3778–3787.
20 M. F. Lichterman, M. R. Shaner, S. G. Handler, B. S. Brunschwig, H. B. Gray, N. S. Lewis and J. M. Spurgeon, *J. Phys. Chem.Lett.*, 2013, **4**, 4188–4191.